The effect of surface chemistry on the performances of Pd-based catalysts supported on activated carbons

UNIVERSITÀ DEGLI STUDI DI TORINO

The effect of surface chemistry on the performances of Pd-based catalysts supported on activated carbons

A. Lazzarini,[a,b] R. Pellegrini,[c] A. Piovano,[d] S. Rudić,[e] C. Castan-Guerrero,[f] P. Torelli,[f] M. R. Chierotti,[a] R. Gobetto,[a] C. Lamberti,[a,g] E. Groppo[a,†]

In this work we investigated in details the effects of nitric acid on the surface chemistry of two carbons, activated by steam and by phosphoric acid, meant to identify the nature and the concentration of the oxidized surface species. To this aim, the oxidized carbons were characterized by means of a large number of complementary techniques, including micro-Raman spectroscopy, N_2 physisorption, Boehm titration method, ^{13}C Solid State Nuclear Magnetic Resonance, X-ray Photoelectron Spectroscopy, Diffuse Reflectance Infrared and Inelastic Neutron Scattering spectroscopies. Carboxylic and carboxylate groups are mainly formed, the latter stabilized by the extended conjugation of the π electrons and more abundant on small and irregular graphitic plateletes. We demonstrated that the presence of oxygen-containing groups acts against the palladium dispersion and causes the appearance of an appreciable induction time in hydrogenation reactions. A carbon with more oxygenated surface species (and in particular more carboxylate groups) has to be favoured in the hydrogenation of polar substrates, while it is detrimental to hydrogenate unpolar substrates

.

1. INTRODUCTION

Activated carbons are widely used as catalysts' supports or even as catalysts on their own. The catalytic performances are strongly influenced by both physical properties (such as surface area and porosity), as well as by the surface chemistry, that is by the nature, concentration and accessibility of the active sites. Indeed, the surface functional groups are capable of chemisorbing the reactants,[1] influence the formation of surface intermediates and determine the wettability of the carbon in different solvents.[2] Chemisorbed oxygen, in particular, plays a fundamental role in determining many properties of carbon-based materials.[3] For activated carbons, which consist mainly of sp^2-hybridized carbon atoms organized in heterogeneous graphene layers, chemisorbed oxygen is predominantly located at the edges of such layers, which are by far more reactive than the basal planes. Oxygenated functionalities are spontaneously formed by exposure of the carbon to the atmosphere after the pyrolysis step, especially in the presence of water and at high temperature. On the other side, controlled thermal treatments at increasing temperature can be used to selectively remove a fraction of these groups, thus tuning the carbon properties.[4,5]

In most of the cases, oxygen containing groups behave as weak acid or basis. Acid groups (among which carboxylic acids and anhydrides, lactones and phenols) are generally formed at the edges of the graphene layers. Their presence makes the carbon more hydrophilic and decreases the electronic density of the basal planes, with a consequent decrease of the basicity of the surface.[4,6-10] Other oxygen functions are considered neutral (such as carbonyls and ethers) or basic (such as quinone, chromene and pyrone groups).[2] The types and the relative abundance of the oxygen functional groups depend on both the origin of the carbon and the activation procedure. For example, activation with phosphoric acid leads to a more pronounced oxidation than activation with steam.[11] Alternatively, the surface chemistry of carbons may be changed by treating them in an oxidative environment, either in the gas phase or in solution. The most common liquid oxidants are nitric acid, hydrogen peroxide and hypochlorite. In particular, oxidation with nitric acid allows a fine tuning of the carbon properties by controlling the acid concentration and the temperature of the treatment. The most accepted oxidation mechanism in the presence of nitric acid has analogies to the oxidation of aromatic hydrocarbons and involves the aliphatic chains at the borders of the graphene layers.[12] When the aliphatic side chains consist of more than one carbon atom, dicarboxylic groups are formed. When one CH_2 group is present between two aromatic rings, the oxidation leads to a ketone group. Additional mechanisms explain the formation of other acidic functional groups at the carbon surface.

The effect of treatments in nitric acids on the surface chemistry of activated carbons has been the subject of many investigations aimed to identify the nature and the concentration of the acidic groups formed at the carbon surface. The topic is gaining attention also in the literature related to carbon nanotubes and graphene materials, since treatments in HNO_3 are largely used as methods to purify and functionalize carbon-based materials for advanced applications.[13-16] A very large number of characterization techniques have been employed to this purpose. The acidic and basic oxygen functions have been traditionally quantified by titration methods,[17] which however fail to reveal the neutral oxygen species. Also FT-IR spectroscopy (mainly in the DRIFT mode) and X-ray Photoelectron Spectroscopy (XPS) have been largely used for qualitative and quantitative purpose. The main defect of both techniques is that they require a curve fitting, which is often complicated by the bands width and the

overlap of many contributions, not always assignable in a univocal way. Finally, temperature programmed desorption (TPD) methods have been used to discriminate the different functional groups as a function of the decomposition temperature and products, but also in this case the results are not always unambiguous.[3] Raman spectroscopy and XRPD techniques have been recently employed to monitor the structural changes induced on carbons by treatments in nitric acid.[18,19]

The emerging scenario is quite complex and the literature on the topic is extremely heterogeneous (if not in conflict).[20] The inconsistencies are mainly due to the diversity of the starting activated carbons (or CNTs or graphene) and to the fact that the treatment conditions (e.g. type and concentration of the oxidizing agent, temperature, treatment duration, and others) differ largely from one author to another. For example, it has been reported that liquid phase oxidation does not change significantly the texture (surface area and porosity) of the activated carbons[9,21-23] but also the opposite, that is, the formation of oxygen containing groups results in the partial blockage of the entrance of micro-pores.[18,24] Very recently, it has been demonstrated that the treatment in nitric acid may cause a partial graphitization of activated carbons, i.e. an increase in the structural and electronic order,[19] although other works do not reveal important structural changes after liquid phase oxidation. Finally, although there is a general consensus on that treatment in nitric acid is the most effective one to make carbons acidic, the types and the concentration of the formed functional groups differ from one work to another. Some authors reported that, besides oxygen-containing groups, also small amounts of nitrogen species are formed by aromatic nitration,[25] especially in the presence of phosphorous groups present in some chemically activated carbons.[11] For MWCNTs, a wet chemical purification in the presence of HNO_3 has been found to change their nature from hydrophobic to hydrophilic, a proof that a certain fraction of functional groups are added at the surface.[13]

The surface chemistry of activated carbons plays a fundamental role in catalysis, both when carbons are used as catalysts and when they are used as supports. For example, interesting activity correlations have been established between the surface chemistry of activated carbons and their catalytic performances in various reactions in the gas phase or in the liquid phase.[2] The surface functional groups in activated carbons have a main role in the different phases of the preparation of metal supported catalysts (e.g. impregnation/deposition of the metal phase, pre-reduction, etc.). For Pd and Pt based catalysts it has been demonstrated that the metal dispersion might be promoted by the presence of a limited amount of surface oxygen groups, which enhance the hydrophilicity and hence improve the access of the metal salt solution during the impregnation step.[23,24,26] However, it has been also noticed that a too high amount of oxygen-containing groups may have the opposite effect on the metal dispersion.[23,24] The presence of surface oxygenated functional groups is known to negatively affect the reducing ability of activated carbons, i.e. the support becomes less reducing in presence of large amounts of oxygen groups.[23] It is also well known that agglomeration of metal nanoparticles can easily occur on activated carbons with a high concentration of carboxylic groups, due to the instability of these groups during the high temperature reduction.[23,24,27-29]

Despite the presence of an abundant and very heterogeneous literature, it is often difficult to distinguish the contribution of the surface chemistry of activated carbons to the overall catalytic performances. Indeed, modification of the carbon surface is often accompanied by textural changes and by variations of the active metal phase, the three phenomena being difficult to separate. Hence, a systematic investigation on the surface properties of a series of activated carbons and related catalysts characterized by similar texture and dispersion of the active phase is timely and crucial in view of rationalizing the behaviour of catalysts prepared on different carbons. Herein, we propose a comprehensive investigation by means of a multi-technique approach[30] of the surface chemistry of two carbons, activated by steam and by phosphoric acid (the two most common methods for carbon activation) and successively treated in oxidising conditions. These carbons were successively used as supports for Pd-based catalysts and further tested in different hydrogenation reactions. In some conditions, the palladium dispersion was not affected by the presence of the acid groups, and hence it was possible to compare the catalytic performances of catalysts having almost the same surface area and porosity, a very similar metal dispersion, but different carbon surface properties, which is a condition rarely found in the literature. We wish to underline here that the focus of the manuscript is on the characterization of the carbon supports more than of the palladium phase. The whole set of data shown in this work allowed us to rationalize, at least in part, the role of carbon surface chemistry in industrially relevant reactions catalysed by metal-supported catalysts.

2. MATERIALS AND METHODS

2.1 Carbon materials

The samples analysed in this work were obtained starting from two types of activated carbons of wood origin, extensively investigated in our previous work,[30] and widely used as supports for metal-supported catalysts of industrial interest. Sample **1** (C_{Chemi} in our previous work) was activated in the presence of H_3PO_4, while sample **2** (C_W in our previous work) was activated by steam. The ash content in the two carbons is very low (below 2 wt%), as determined by calcination, and thus they are not considered to take part in the surface chemistry.

The two carbons were oxidized with concentrated HNO_3 (67% w/w) at room temperature for 24 hours, and successively washed with distilled water until the washing solution reached a pH = 7, resulting in samples **1a** and **2a**. For comparison, sample **2** was also oxidized in H_2O_2 at room temperature for 24 hours, resulting in sample **2b**. Table 1 summarizes all the samples investigated in the work, the corresponding specific

surface area and micropores volume as determined by N_2 physisorption measurements (vide infra), and the total acidity evaluated by Boehm titration method (vide infra).

2.2 Carbons characterization methods

2.2.1 N_2 physisorption at 77 K. The specific surface area and pore volume of all the carbons in Table 1 were measured by N_2 physisorption at 77 K. The measurements were performed on a Micromeritics ASAP 2020 instrument. The adsorption isotherms were analysed according to the procedure described in Ref. [31].

2.2.2 Titration of the total acidic surface functions. The carbons were titrated with sodium hydroxide solution to determine their total acidity capacity, as suggested by Boehm.[17] 0.3 grams of each carbon were placed in separate plastic bottles, and then 25 ml of 0.05 M NaOH solution was added. The bottles were gently shaken for 48 hours, and the solutions were then filtered. The amount of NaOH adsorbed by each carbon was determined by back titration of the solution with a standardized HCl solution.

2.2.3 SSNMR spectroscopy. ^{13}C SSNMR spectra were recorded on a Bruker Avance II 400 instrument working at 100.65 MHz. The samples were measured inside cylindrical zirconia rotors (diameter = 4 mm, sample volume = 80 µl) spun at 12 kHz, employing the Ramp-Amplitude Cross-Polarization pulse sequence (^1H 90° pulse = 3.05 µs, contact time = 1.5 ms, relaxation delay 0.2 s) with the Two Pulse Phase Modulation ^1H decoupling with an rf field of 75 kHz during the acquisition period. A DEPTH sequence ($\pi/2$ - π - π) for the suppression of the probe background signal was used. ^{13}C chemical shifts were referenced with the resonance of glycine (^{13}C methylene signal at 43.86 ppm) as external standard.

2.2.4 Raman spectroscopy. Raman spectra were recorded by using a Renishaw inVia Raman microscope instrument, with an excitation λ = 514 nm, and the laser power fixed at 0.5 % of the total. The photons scattered by the sample were dispersed by a 1800 lines/mm grating monochromator and simultaneously collected on a CCD camera; the collection optic was set at 20X objective. The spectra were obtained by collecting 20 acquisitions (each of 50 s) on samples in the powder form.

2.2.3 XPS spectroscopy. High resolution XPS spectra were collected in the ultra-high vacuum chamber (base pressure $3 \cdot 10^{-10}$ mbar) of the APE beamline at the ELETTRA synchrotron radiation facility (Trieste, Italy).[32] The samples were pressed in the form of powder on an indium foil to ensure mechanical and electrical contact with the Mo sample-holder. During measurements, the photon energy was set to 780 eV. The light was linearly polarized and was impinging on the sample at an angle of 45 degrees with the surface. The spectra were all collected at normal emission and room temperature. The overall energy resolution has been estimated to be about 0.3 eV. The Au4f of a gold foil reference was periodically acquired to monitor the photon energy. All the spectra were aligned by shifting the spectra to fix the maximum of the $Au4f_{7/2}$ to 84 eV of binding energy. The XPS analysis is always extremely surface sensitive and the main contribution comes from the firsts atomic planes. The background was approximated by a third-order polynomial function combined with the Shirley model for inelastic processes and subtracted from the original spectra. The C1s spectra were deconvoluted by using 7 pseudo-Voigt peaks, following the improved method suggested by Smith et al. [33]

Table 1. List of the activated carbons investigated in this work as a function of the type of activation and post treatment in oxidizing conditions, corresponding specific surface area and volume of the micropores (as determined by N_2 physisorption measurements) and total acidity (as determined by the Bohem titration method).

Entry	Activation	Post Treatment	SA_{BET} (m^2/g)	V_{micro} (cm^3/g)	Total Acidity (meq/g)
1	H_3PO_4	-	1508	1.11	0.42
1a		1 + HNO_3	1442	1.13	1.51
2	Steam	-	1018	0.63	0.16
2a		2 + HNO_3	949	0.59	0.92
2b		2 + H_2O_2	967	0.63	0.33

2.2.5 DRIFT spectroscopy. DRIFT spectra were collected on a Nicolet 6700 instrument equipped with a ThermoFisher Smart accessory and a MCT detector. The spectra were collected at 4 cm^{-1} resolution and averaging 1024 scans. The measurements were performed on powdered samples in air, without dilution in KBr. The spectra were collected in reflectance and successively converted in Kubelka-Munk units (K.M.).

2.2.6 INS spectroscopy. The INS spectra were recorded at the TOSCA spectrometer at the ISIS spallation neutron source (Rutherford Appleton Laboratory, UK).[34] The samples were previously treated in vacuum at 150 °C for a prolonged time in order to remove the physisorbed water. Successively, they were inserted in a thin aluminium envelope and then placed into In-wire sealed Al cells. All the manipulations were performed inside a glove-box to prevent contamination by moisture. Finally, the cell was inserted in a duplex CCR cryostat, and the measurements were performed at 20 K. Each INS spectrum was measured with a high statistic, by integrating for 1500 µA of the proton current (proton accelerator was working at about 150 µA/hour). The signal from detectors both in forward and in backward directions have been extracted and combined using Mantid software,[35] without any sign of degradation of the resolution. The beam size was 40 mm x 40 mm so that a representative macroscopic amount (approximately 8 grams) of samples was measured in each experiment. Since the intensity of the INS signal is proportional to the amount of the corresponding chemical species, the spectra were normalized on sample mass and incoming proton current values in order to allow a quantitative comparison among the samples.

2.3 Catalysts preparation and characterization

Pd/C catalysts (5 wt% Pd loading) were prepared in the Chimet S.p.A. laboratories[36] on some of the carbons reported in Table 1, following the deposition-precipitation method as reported elsewhere,[31,37] using Na_2PdCl_4 as the metal precursor and Na_2CO_3 as the basic agent and changing other experimental variables, such as pH and temperature according to

proprietary protocols. All the catalysts were water washed in order to remove residual chlorine and dried at 120 °C overnight. The catalysts were used without performing a pre-reduction step, meaning that the reduction of the Pd phase occurs during the reaction. The metal dispersion was evaluated by means of CO chemisorption method. The measurements were performed at 50 °C by a dynamic pulse method on samples pre-reduced in H_2 at 120 °C.[38] Typically, the catalyst (200 mg) is loaded inside the U-tube, heated in He up to 120 °C (at 10 °C min^{-1}), reduced in H_2 for 30 min, and finally cooled down to 50 °C in He (at 10 °C min^{-1}). A CO/metal average stoichiometry of 1 was assumed to calculate the metal dispersion, as suggested in the literature.[39,40]

The complete list of the examined catalysts, their reduction state, the Pd dispersion (determined by CO chemisorption experiments), and the catalytic performances in terms of activity and induction time in two hydrogenation reactions are summarized in Table 2.

2.4 Catalytic performances in hydrogenation reactions

2.4.1 Debenzylation of 4-benzyloxyphenol to hydroquinone and toluene. The reaction was carried out according to the procedure reported in Ref. [41]. Briefly, 500 mg of dry catalyst were charged in 300 cm^3 glass reactor equipped with a double mantle for water circulation and a gas injection stirrer (Premex, br1 series), together with a solution of 10 g of 4-benzyloxyphenol in 140 ml of ethanol. After purging the reactor with nitrogen, hydrogen was introduced. The reaction was performed at atmospheric pressure, at a temperature of 35 °C, and with a stirring speed of 2000 rpm. It was demonstrated that the reaction has a zero order with respect to the substrate and, in the adopted experimental conditions, it proceeds without mass transfer constraints.[42]

2.4.2 Hydrogenation of methylcyclohexene. By using the same equipment and procedure described above, 3.5 g of 1-methyl–1-cyclohexene in 150 ml of ethanol were hydrogenated by using 100 mg of dry catalyst. The reaction was performed at atmospheric pressure, at a temperature of 30 °C, and with a stirring speed of 2000 rpm.

3. RESULTS AND DISCUSSION

3.1 Effects of HNO_3 treatment on the textural and structural properties of activated carbons

The textural properties of all the carbons examined in this work are summarized in Table 1. For both carbons **1** and **2**, the treatment in HNO_3 has no significant impact on the texture. Only a slight decrease of the specific surface area is observed in both cases, which is however within the experimental error (below 7%). Oxidation of carbon **2** in H_2O_2 has even smaller effect. It is interesting to observe that greater textural variations have been reported in the literature when oxidation is carried out in concentrated HNO_3.[18,24] However, in most of the cases the treatments are performed at higher temperature, while in our case it is conducted at room temperature. Not only the texture, but also the microstructure of the two activated carbons is almost unaffected by the oxidation treatment. Raman spectroscopy (Figure S1 and Figure S2) indicates only a subtle increase of the graphitic order for the oxidized carbons, in agreement with the recent work of Collins et al.[19]

Table 2. List of the carbon-supported Pd-based catalysts investigated in this work. For each catalyst, the following data are reported: the type of carbon used as support and the metal dispersion evaluated by CO chemisorption method (on samples pre-reduced in H_2 at 120 °C). Moreover, the catalytic performances of each catalyst in two hydrogenation reactions are also reported, in terms of induction time, activity and turnover frequency (TOF).

Label	Carbon type	D (%)	BOP debenzylation			MCHe hydrogenation		
			Induction time (min)	Activity (cm^3/min)	TOF (s^{-1})	Induction time (min)	Activity (cm^3/min)	TOF (s^{-1})
A	**1**	26.9	2.8	19.9	0.218	2.0	50.3	2.757
B	**1**	18.8	0.3	21.5	0.337	0.4	29.0	2.274
C	**1**	17.1	0.3	15.0	0.258	0.2	38.7	3.330
D	**1a**	16.5	16.0	38.1	0.683	22.0	11.2	1.003
E	**2**	25.5	0	15.5	0.179	0.4	45.7	2.642
F	**2**	36.1	0	16.1	0.131	0.2	44.0	1.800
G	**2**	33.3	0	19.0	0.168	0.3	47.5	2.103
H	**2a**	31.7	6.2	15.7	0.146	0.7	40.7	1.893

3.2 Effects of HNO_3 treatment on the surface chemistry of activated carbons

The total amount of acid functions at the carbons surface was determined by titration, following the Boehm method and using NaOH as titrating agent. NaOH is classically regarded as an approximate probe of carboxyl, lactonic and phenolic groups.[17,43] The results are summarized in Table 1. Carbon **1**,

activated by H_3PO_4, contains more than the double of total acid groups than carbon **2**, activated by steam. The treatment in nitric acid causes a significant increase of the total acidity of both carbons **1** and **2**. In percentage, the increase is grater for carbon **2** (6-fold increase) than for carbon **1** (about 4-fold increase). H_2O_2 reveals to be much less effective than HNO_3 in introducing acid functions. Indeed, carbon **2b** simply shows the double of acid groups with respect to its parent **2**.

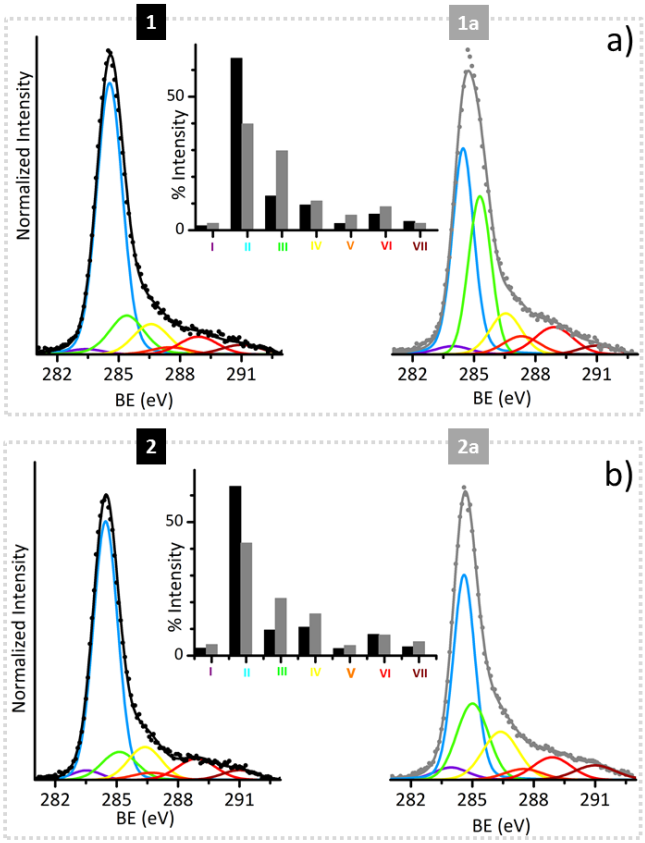

Figure 1. High resolution C1s XPS spectra for carbons **1** – **1a** (part a) and **2** – **2a** (part b). The corresponding fits with seven Gaussian components are also reported. Black, dark grey and light dots and lines refer to experimental and the best-fit curves, respectively. The insets show the distribution of carbon among different chemical states. Peak intensities are expressed as percentage with respect to the total normalized intensity of the C1s peak of the XPS spectrum.

The types, concentration and location of the surface functional groups have been successively investigated by means of multiple spectroscopic techniques. Figure 1 shows the high resolution C1s XPS spectra of carbons **1** – **1a** (Figure 1a) and **2** – **2a** (Figure 1b). In both cases, the spectra change after the oxidation treatment. In particular, the dominant peak becomes broader and shifts at higher binding energy. At the same time, the tail at high binding energy becomes progressively more pronounced, indicating the presence of several oxygen containing species. To accurately assign the C1s region a variety of deconvolution schemes have been proposed in the past,[44-51] recently debated,[33,52] and improved[33] to account for the presence of disordered carbon and surface defects, which have to be considered when analysing potentially defective surfaces of graphitic carbon. We have followed the improved deconvolution method proposed very recently by Smith et al.,[33] which involves the use of seven peaks (insets in Figure 1). The primary C-C peak (peak II) is assigned to graphitic sp^2 carbons. The remaining two C-C peaks, centred near 283.8 eV (peak I) and 285 eV (peak III), are assigned to defects.[33,52] The region of oxygenated carbon consists of three contributions, centred at approximately 286.2 eV (C-O, peak IV), 287.5 eV (C=O or O-C-O, peak V) and 289 eV (O=C-O, curve peak VI). Finally, the π-π* shake-up peak (peak VII) contributes around 291.5 eV.

The results of the deconvolution are summarized in the insets of Figure 1. The most evident change by going from sample **1** to sample **1a** is a drastic decrease in intensity of the predominant C-C peak (peak II), accompanied by an increase of peaks I and III, associated to defective sp^2 carbons. Peak III is the most affected, increasing by more than the double. The origin of this peak has been very recently attributed to long range effects of oxygenated species on non-adjacent carbons.[33,52] Concurrently, peaks IV, V and VI increase in intensity, indicating that the treatment in HNO_3 causes a partial oxidation of the carbon. In particular, peak V (attributed to carbonyl groups and carbons attached to two ether/hydroxyl groups) and peak VI (assigned to carboxyl, lactone and ester groups) are the most affected. A similar behaviour is observed for carbon **2** albeit the relative proportion of the oxygen-containing groups is slightly different.

Complementary information on the nature of the surface functional groups were obtained by vibrational spectroscopies. The DRIFT spectra of carbons **1** and **2** (Figure 2) are dominated by two main absorption bands:[30] 1) a narrow band around 1600 cm^{-1}, which is due to the ν(C=C) vibrational modes of conjugated sp^2 bonds belonging to graphitic islands,[53] enhanced by the presence of oxygen atoms, and 2) a very broad absorption in the 1300 – 1000 cm^{-1} region due to the overlapped contribution of C–H in-plane bending modes and of the collective skeletal C-C vibrational modes.[53,54] The surface functional groups contribute at the two extremes of the spectrum. In particular, the weak band around 1710 cm^{-1} is assigned to ν(C=O) vibrations of carboxyl and carbonyl groups. Moreover, the series of bands in the 900 - 750 cm^{-1} range are

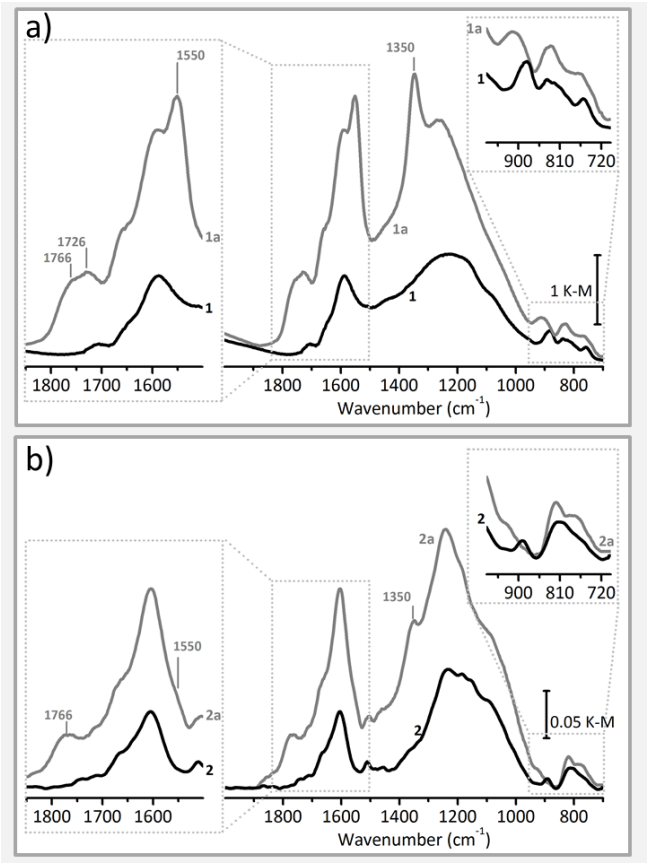

Figure 2. DRIFT spectra of carbons **1** – **1a** (part a) and **2** – **2a** (part b). The insets show a magnification of the spectral regions corresponding to ν(C=O) and out-of-plane C-H bending vibrations, respectively.

assigned to the out-of-plane vibrations of C-H species at the borders of the sp^2 domains, differing in the number of adjacent H atoms.[54] The DRIFT spectrum of carbon **2** is much less intense than that of carbon **1**, as a consequence of the smaller amount of surface functional groups and of the greater graphitic character. Moreover, the band around 1710 cm^{-1} is almost negligible, in good agreement with the lower amount of acid groups titrated with NaOH (Table 1).

The DRIFT spectra of the oxidized carbons **1a** and **2a** are much more intense (almost doubled) than those of the parents **1** and **2**, which is a direct consequence of the increased dipole moment associated with the sp^2 ring vibrations, as expected in the presence of oxygenated electron-withdrawing groups. In addition, new absorption bands are observed, denoting the formation of new functional groups, as follows.

A first group of bands appear in the ν(C=O) vibrational region, with absorption maxima at 1766 and 1726 cm^{-1} for carbon **1a** and at 1766 cm^{-1} for carbon **2a**. The appearance of these bands witnesses the formation of acidic functionalities. Indeed, most of the oxygen containing groups at the surface of activated carbons are characterized by ν(C=O) vibrations close to 1700 cm^{-1}, while they differ in the position of the ν(C-C-O) and ν(C-O) vibrations. Similar absorption bands are observed in the spectra of graphene oxide or partially reduced graphene oxide.[55-57] Attempts to deconvolve this spectral region and to assign each component to a specific functional group are abundant in the literature, and the assignments are often contradictory. The interpretation is difficult also because the ν(C=O) vibrations of acid groups in an aromatic ring structure are affected by the presence of different peripheral groups in close proximity. Hence, the same band can be potentially ascribed to two different groups, or to the same one but in two different environments. However, only the band at 1766 cm^{-1} was affected after neutralization with Na_2CO_3, with the concomitant appearance of two bands around 1610 and 1460 cm^{-1} (not shown). Hence, this band is univocally assigned to carboxylic groups (i.e. COOH), that are converted to carboxylates (i.e. COO^-Na^+) in the presence of Na_2CO_3. Notably, the ^{13}C CPMAS NMR spectra of both carbons **1a** and **2a** (Figures S3 and S4) distinctly show a peak around 180 ppm, which indicates the presence of C=O functional groups, most likely carboxylic rather than carbonyl groups. The C=O signal in the spectrum of carbons **1a** and **2a** are slightly different, suggesting a different population of the functional groups, with **1a** being more populated than **2a**.

A second group of bands appear at 1550 cm^{-1} and 1350 cm^{-1}. We assign these bands to the asymmetric and symmetric stretching modes of carboxylate groups (formally COO^-). The assignment is corroborated by the insensitivity of these bands to the treatment with Na_2CO_3 (not shown).[58] Absorption bands in very similar positions have been observed in the IR spectra of graphene oxide (GO) and reduced graphene oxide (r-GO) at pH values higher than 4.0.[56] The formation of carboxylates in acidic conditions is made possible because of the extended conjugation of the π electrons, which allows a redistribution of the electron density within the graphene layers. It has been demonstrated that for aromatic acids both inductive effects (i.e. the influence of neighbours on the acidic strength of carboxylic groups) and resonance effects contribute to enhancing the stability of carboxylate anions.[9] This phenomenon has been recently discussed by Collins et al.[19] as responsible for the partial graphitization of activated carbons by HNO_3 treatments. It is interesting to observe that these bands dominate the spectrum of carbon **1a**, while they are scarcely observed in the spectrum of carbon **2a**. Carbon **1a** is characterized by graphitic domains smaller and more irregular than carbon **2a**. Moreover, it contains a much larger number of additional functional groups. Similar absorption bands are observed in the spectra of graphene oxide or partially reduced graphene oxide in stabilizing the carboxylate anions by intramolecular hydrogen bonding.[56] Recently, this effect has been accounted for explaining the superior water dispersibility of GO with respect to r-GO.[56] On these bases, we can conclude that the COO^- carboxylate groups are better stabilized on activated carbons characterized by small sp^2 domains and by the presence of additional oxygen-containing functionalities.

Finally, the treatment in HNO_3 causes also a modification of the C-H terminal groups. This is revealed by the modification of the DRIFT spectrum in the 900 – 750 cm^{-1} region (insets in Figure 2). In particular, the absorption band at 880 cm^{-1} (*solo* species) shift to 912 cm^{-1}, the couple of bands at 838 – 807 cm^{-1} (assigned to *duo* and *trio* species) is transformed in a

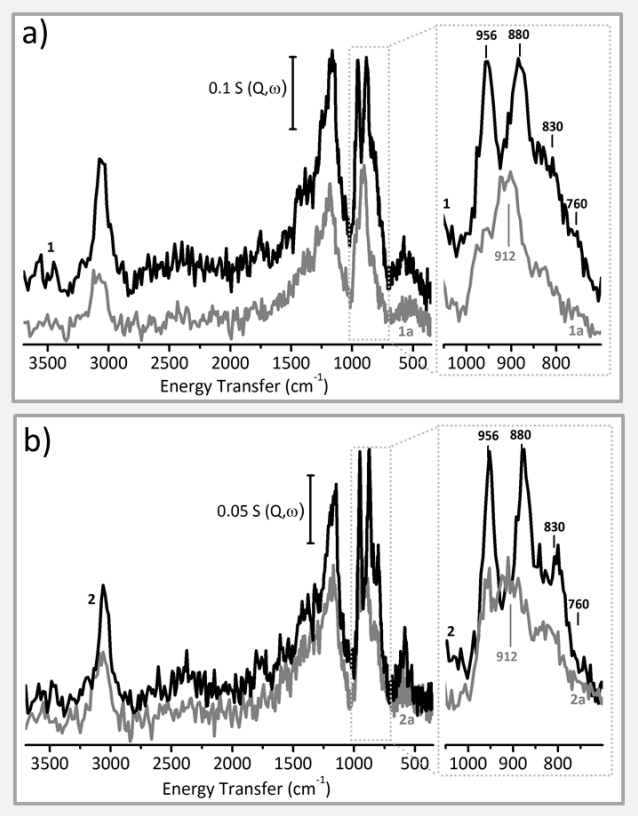

Figure 3. INS spectra of carbons **1** – **1a** (part a) and **2** – **2a**. The insets show a magnification of the spectral region corresponding to the out-of-plane C-H bending vibrations.

single band centred at 830 cm^{-1}, and the band at 758 cm^{-1} (assigned to *duo* and *trio* species) shifts upward to 765 cm^{-1}.

Additional and complementary insights on the H-containing functional groups present at the surface of the modified carbons are provided by INS spectroscopy. Indeed, INS is the technique of choice to observe the vibrations due to the hydrogen terminations at the borders of the sp^2 domains, because the neutron cross-section for hydrogen nuclei is one order of magnitude larger with respect to all other elements.[30] The INS spectra of carbons **1** – **1a** and **2** – **2a** are shown in Figure 3. All the bands observed in the spectra are ascribable to vibrational modes involving a large hydrogen displacement from the rest position.[30] The band around 3060 cm^{-1} is due to ν(C-H) vibrations, while those around 1200 cm^{-1} and in the 800 – 1000 cm^{-1} region are due to the in-plane and out-of-plane C-H bending modes of the hydrogen species belonging to condensed rings edges.[59] Finally, the weak bands in the 700 - 400 cm^{-1} region are mainly due to C-C torsion modes of the carbon atoms at the edge of the graphene layers, which indirectly cause a substantial movement of the hydrogen atoms (riding vibrations).[60]

The spectra of carbons **1a** and **2a** are less intense than those of the parents **1** and **2**. Since the spectra are normalized to the sample mass and hence the intensity of each band is directly proportional to the quantity of the corresponding species, the lower intensity indicates that a fraction of the hydrogen terminations has been consumed in favour of the new oxygenated functional groups. Curiously, the phenomenon is opposite to that observed in DRIFT, where treatment in HNO_3 of the carbon causes an overall increase of the spectral intensity, because of the increased dipole moment associated with the sp^2 ring vibrations (Figure 2). The main differences after the oxidation treatment are observed in the low frequency region of the spectra, and reflect the changes previously observed in the DRIFT spectra (Figure 2), with some additional details. Indeed, INS spectroscopy is not subjected to selection rules, as DRIFT spectroscopy, and all the vibrational modes are visible. The absorption bands at 956 cm^{-1}, absent in the DRIFT spectra and assigned to the vibrations of *duo* and *trio* C-H species at irregular borders,[30,60] significantly decreases in intensity, as well as the bands at 830 and 760 cm^{-1}, also due to *duo* and *trio* C-H species. In contrast, the band at 880 cm^{-1}, assigned to the vibrations of *solo* C-H species at regular extended borders,[30,60] is almost unaffected in intensity but upward shift to 912 cm^{-1}. These results indicate that the treatment in HNO_3 affects mainly the irregular borders of the graphene layers, which are likely attacked by the oxygenated functional groups. However, the presence of these electron-withdrawing species at the irregular borders has indirect consequences also on the regular extended edges, as reflected by the substantial shift of the band associated to the vibrations of the corresponding C-H terminations.[61]

3.3 Consequences on the catalytic performances

Carbons **1**, **1a**, **2** and **2a** have been used as supports for Pd-based catalysts, prepared following different experimental protocols as described in Section 2.3, and tested in two hydrogenation reactions, namely the debenzylation of 4-benzyloxyphenol (BOP) to hydroquinone and toluene, and the hydrogenation of methylcyclohexene (MCHe) to methylcyclohexane, both of them conducted in alcoholic solvent. The complete list of the examined catalysts, the Pd dispersion, and the catalytic performances in terms of activity, turnover frequency (TOF) and induction time in the two above mentioned reactions are summarized in Table 2. We wish to underline that in this work the Pd dispersion has been determined by means of CO chemisorption, which measures the number of adsorbed CO molecules and, under the assumption of a defined CO/Pd stoichiometry, provides the fraction of available surface Pd atoms. In a previous paper of this series[42] we have demonstrated that, for carbon-supported Pd-based catalysts prepared following proprietary protocols analogous to those adopted in this work, the dispersion values obtained by CO chemisorption are in very well agreement with those independently determined by SAXS (which gives a particle size distribution of the whole particle population) and by TEM. We also demonstrated that the exposure of the catalysts to the reaction conditions does not cause any change in both the particle size and aggregation degree.[42] With respect to TEM, that intrinsically suffers of a limited statistical representability, CO chemisorption method has the advantage to measure all the accessible Pd sites.[39] Moreover, being widely available and relatively fast, it is the technique of choice for screening the metal dispersion of a larger number of

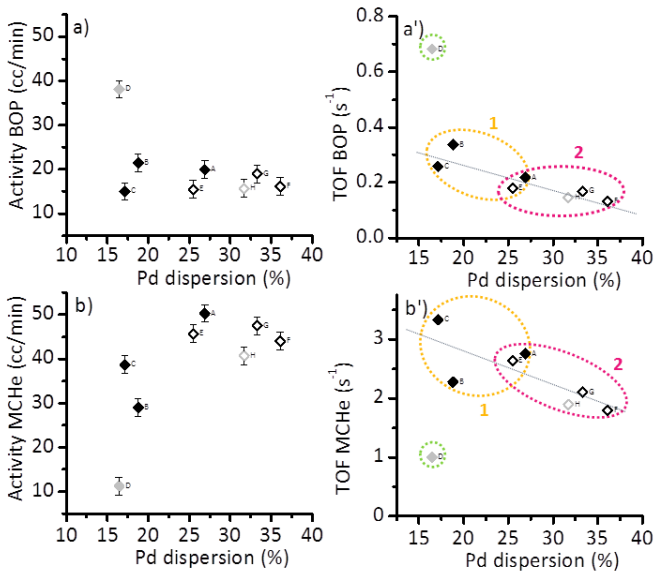

Figure 4. Catalytic activity of a series of Pd-based catalysts supported on carbons **1**, **1a**, **2** and **2a** in the debenzylation of 4-benzyloxyphenol (BOP) to hydroquinone and toluene (part a) and in the hydrogenation of methylcyclohexene (MCHe) to methylcyclohexane (part b), as a function of the Pd dispersion. Full black, full grey, empty black and empty grey symbols refer to catalysts supported on carbons **1**, **1a**, **2**, and **2a** respectively. Parts a' and b' show the same data reported in terms of turnover frequency values (TOF). Yellow, pink and green circles highlight the catalysts on carbons of types **1**, **2** and **1a**, respectively. The grey light is a guide for eyes highlighting the almost linear relation between TOF and metal dispersion.

catalysts as in the present work. Finally, the TOF values were calculated by assuming that all the accessible Pd sites (as determined by CO chemisorption) are active. Hence, the TOF values have to be considered as inferior limits.

We have demonstrated previously that activated carbons are rather inert toward deposition–precipitation of the Pd phase. The variations of surface area and pore volume were negligible,[41] and no changes in the structural and surface properties were observed, except for the consumption of a minority of the C–H terminations which are likely involved in the deposition of the active phase.[30] Hence, it is reasonable to assume that the surface properties discussed in the section above for the carbon supports hold also for the corresponding catalysts.

According to Table 2, the catalysts prepared with carbons of type **1** usually show a metal dispersion lower than those prepared with carbons of type **2**. Catalyst **D**, having carbon **1a** as support, is showing the lowest dispersion. These data suggest that, with the synthetic protocols adopted in this work, the oxygen-containing surface functional groups act against the metal dispersion, in agreement with a fraction of the literature.[23,24] The catalysts on carbons of type **1** always showed an induction time before the reaction starting, irrespective of the considered reaction and of the metal dispersion, with catalyst **D** having the longest induction time. Among catalysts of type **2**, only catalyst **H** on carbon **2a** shows an appreciable induction time in both considered reactions. It is worth noticing that similar induction times were observed previously for other hydrogenation reactions performed at atmospheric pressure[41,42] on carbon and alumina supported catalysts. Since it has been demonstrated that in the adopted experimental conditions the reactions proceed without mass transfer constraints, this effect can be attributed mainly to the presence of oxygen-containing groups. The origin of the phenomenon is not clear yet. A possible explanation might invoke an enhancement of the hydrogen spillover effect upon increasing the oxygen content in the carbon, as recently reported in the specialized literature.[62]

As far as the catalytic activity is concerned, Figure 4ab shows the hydrogenation activity in the two reactions as a function of the metal dispersion, while Figure 4a'b' shows the same data expressed in terms of TOF. Irrespective of the metal dispersion, in average catalysts on carbon **1** perform better than those on carbon **2** in the hydrogenation of BOP (Figure 4a). Catalyst **D** on carbon **1a** is the best performing one, also when comparing with catalysts **B** and **C** that have a very similar Pd dispersion. In contrast, the performances of catalyst **H** on carbon **2a** are very similar to those of the other catalysts on carbons of type **2**. The trend is maintained also when the TOF values are plotted as a function of the Pd dispersion (Figure 4a'). If we exclude catalyst **D**, an almost linear correlation is observed, which is indicative of a structure sensitive reaction (i.e. the active catalytic site is formed by several adjacent surface Pd atoms occupying well defined positions, which makes bigger particles more performing than smaller ones), in good agreement with our previous findings.[42] Catalyst **D**, however, escapes from this linear correlation, suggesting that it contains certain surface sites much more active than the other catalysts. We attribute the outstanding performances of catalyst **D** to the peculiar surface chemistry of carbon **1a**. According to the experimental data discussed above, carbon **1a** contains much more carboxylates than all the other carbons. These surface groups are stabilized by a redistribution of the electron density within the graphitic domains. We can conclude that a carbon with more oxygen-containing groups is in general beneficial to structure-sensitive hydrogenation of polar substrates (like BOP), because it decreases the metal dispersion. Moreover, specific surface functional groups (such as carboxylates) more than others, further enhance the catalytic activity.

The opposite behaviour is observed for the hydrogenation of methylcyclohexene. In general, catalysts on carbons of type **1** are less performant in terms of activity than those on carbons of type **2**. However, when the same data are shown in terms of TOF (Figure 4b') the trend changes. As for the debenzylation of BOP, also in this case a linear correlation is observed between TOF and metal dispersion, indicating that also hydrogenation of MCHe is structure sensitive. Again, catalyst **D** escapes from the linear trend, but this time it is the worst one. We can conclude that the same surface properties of carbon **1a** that were beneficial for hydrogenating a polar substrate turn out to be detrimental in the hydrogenation of unpolar substrates. The above discussion holds irrespective of the solvent (which is the same in both reactions).

4. CONCLUSIONS

In this work we present a comprehensive investigation on the surface chemistry of two carbons of wood origin, activated either by phosphoric acid (type **1**) or by steam (type **2**), and successively treated in oxidizing conditions. We demonstrate that the treatment in HNO_3 scarcely affects the morphology and nano-structure of the two carbons (as evidenced by N_2 physisorption and Raman measurements), while it introduces a certain number of oxygen-containing surface functional groups whose nature, relative abundance and location is determined by synergically coupling Bohem titration with ^{13}C SSNMR, C1s XPS, DRIFT and INS spectroscopies. We found that, together with carboxylic and ester groups, carboxylate species are also present, stabilized by the extended conjugation of the π electrons. These oxygen-containing groups are located mainly at the irregular borders of the sp^2 domains, but their presence also largely affects the properties of the C-H groups terminating the regular borders. They are predominantly formed on small and irregular sp^2 graphitic domains, where the negative charge has more chances to be stabilized by the graphene layer. Hence, their contribution becomes relevant for carbons of type **1** (chemically activated), which are intrinsically more defective than carbons of type **2** (activated by steam).

By analysing a large set of catalysts prepared on the same carbons and differing in the preparation procedure, we were able to isolate the contribution of the carbon surface chemistry in determining the performances of carbon-supported Pd-based catalysts in structure-sensitive hydrogenation reactions, in terms of activity, TOF and induction time. A schematic summary of our results is shown in Figure 5. In our experimental conditions, the presence of oxygen-containing functional groups at the carbon surface is responsible of a general decrease of the palladium dispersion and of the appearance of an appreciable induction time in hydrogenation reactions. A catalyst on a carbon with more oxygenated surface species is more active in the hydrogenation of polar substrates, while it is detrimental to hydrogenate unpolar substrates. Certain functional groups at the carbon surface are particularly effective in influencing the catalytic performances. In particular, carboxylate groups enhance/depress the activity in the hydrogenation of polar/unipolar substrates. Part of this effect might be attributed to the redistribution of the electronic charges within the graphitic domains when carboxylates are present at the borders.

Hence, these results indicate a strategy for the preparation of the right carbon-based catalyst to be used in a specific hydrogenation reaction. For the hydrogenation of polar substrates, a carbon characterized by small and irregular sp^2 domains (such as those chemically activated) subjected to an oxidizing post-activation treatment has to be preferred, provided that a long induction time before the starting of the reaction is not a problem. For the hydrogenation of unpolar substrates, instead, a more regular and graphitic carbon (such as those activated by steam) without any further treatment must be selected.

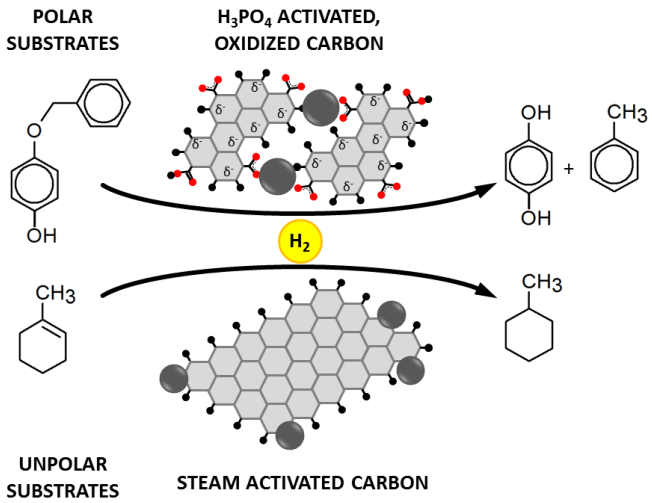

Figure 5. Schematic representation of the strategy to be used for the preparation of the right carbon-based catalyst to be used in a specific hydrogenation reaction.

ACKNOWLEDGEMENTS

We are deeply indebted with the colleagues and friends who contributed to the born of this fascinating story, in particular Giuseppe Leofanti, Giovanni Agostini, Adriano Zecchina and Giuseppe Spoto. We would like to thank Andrea Governini for the catalysts preparation and the catalytic tests, Michele Carosso who has been recently involved in this story and will continue it, and Francesca Bonino and Matteo Signorile for the helpful discussion on the Raman spectra. The XPS measurements have been performed in the framework of the nanoscience foundry and fine analysis (NFFA-MIUR Italy Progetti Internazionali) project. C.L. is grateful for support from the Mega-grant of the Russian Federation Government to support scientific research at the Southern Federal University, No. 14.Y26.31.0001.

Notes and references

1 L. R. Radovic, I. F. Silva, J. I. Ume, J. A. Menéndez, C. A. L. Y. Leon and A. W. Scaroni, *Carbon* 1997, **35**, 1339.
2 J. L. Figueiredo and M. F. R. Pereira, *Catalysis Today* 2010, **150**, 2.
3 H. P. Boehm, *Carbon* 2002, **40**, 145.
4 J. A. Menendez, J. Phillips, B. Xia and L. R. Radovic, *Langmuir* 1996, **12**, 4404.
5 A. Lazzarini, A. Piovano, R. Pellegrini, G. Agostini, S. Rudić, C. Lamberti and E. Groppo, *Physics Procedia* 2016, **85**, 20.
6 S. S. Barton, M. J. B. Evans, E. Halliop and J. A. F. MacDonald, *Carbon* 1997, **35**, 1361.
7 C. Leon, J. M. Solar, V. Calemma and L. R. Radovic, *Carbon* 1992, **30**, 797.
8 M. V. Lopez-Ramon, F. Stoeckli, C. Moreno-Castilla and F. Carrasco-Marin, *Carbon* 1999, **37**, 1215.
9 C. Moreno-Castilla, N. V. Lòpez-Ramòn and F. Carrasco-Marín, *Carbon* 2000, **38**, 1995.
10 B. R. Puri, *Surface complexes on carbons*, in: Chemistry and physics of carbon; Walker, P. L., Ed.; Dekker: New York, **1970**; Vol. Volume 6, p. 191.

11 J. J. Ternero-Hidalgo, J. M. Rosas, J. Palomo, M. J. Valero-Romero, J. Rodríguez-Mirasol and T. Cordero, *Carbon* 2016, **101**, 409.
12 P. Vinke, M. van der Eijk, M. Verbree, A. F. Voskamp and H. van Bekkum, *Carbon* 1994, **32**, 675.
13 L. Stobinski, B. Lesiak, L. Kövér, J. Tóth, S. Biniak, G. Trykowski and J. Judek, *J. Alloy. Comp.* 2010, **501**, 77.
14 L. Ma, X. Yang, L. Gao, M. Lu, C. Guo, Y. Li, Y. Tu and X. Zhu, *Carbon* 2013, **53**, 269.
15 M. Rosillo-Lopez and C. G. Salzmann, *Carbon* 2016, **106**, 56.
16 N. Wester, S. Sainio, T. Palomäki, D. Nordlund, V. K. Singh, L. S. Johansson, J. Koskinen and T. Laurila, *J. Phys. Chem. C* 2017, **121**, 8153.
17 H. P. Boehm, *Chemical Identification of Surface Groups*, in: Advances in Catalysis; Eley, D. D.; Pines, H.; Weisz, P. B., Ed.; Academic Press Inc.: New York, **1966**; Vol. Volume 16, p. 179.
18 J. Collins, T. Ngo, D. Qu and M. Foster, *Carbon* 2013, **57**, 174.
19 J. Collins, D. Zheng, T. Ngo, D. Qu and M. Foster, *Carbon* 2014, **79**, 500.
20 J. Jaramillo, P. M. Álvarez and V. Gómez-Serrano, *Fuel Processing Technology* 2010, **91**, 1768.
21 J. P. Chen and S. Wu, *Langmuir* 2004, **20**, 2233.
22 J. L. Figueiredo, M. F. R. Pereira, M. M. A. Freitas and J. J. M. Órfão, *Carbon* 1999, **37**, 1379.
23 T. Gong, L. Qin, W. Zhang, H. Wan, J. Lu and H. Feng, *The Journal of Physical Chemistry C* 2015, **119**, 11544.
24 J. Li, L. Ma, X. Li, C. Lu and H. Liu, *Industrial & Engineering Chemistry Research* 2005, **44**, 5478.
25 J. P. S. Sousa, M. F. R. Pereira and J. L. Figueiredo, *Catalysis Today* 2011, **176**, 383.
26 F. Rodríguez-Reinoso, *Carbon* 1998, **36**, 159.
27 F. Coloma, A. Sepulveda-Escribano, J. L. G. Fierro and F. Rodriguez-Reinoso, *Langmuir* 1994, **10**, 750.
28 M. C. Román-Martínez, D. Cazorla-Amorós, A. Linares-Solano, C. S.-M. n. De Lecea, H. Yamashita and M. Anpo, *Carbon* 1995, **33**, 3.
29 D. J. Suh, T. J. Park and S. K. Ihm, *Industrial & Engineering Chemistry Research* 1992, **31**, 1849.
30 A. Lazzarini, A. Piovano, R. Pellegrini, G. Leofanti, G. Agostini, S. Rudić, M. R. Chierotti, R. Gobetto, A. Battiato, G. Spoto, A. Zecchina, C. Lamberti and E. Groppo, *Catalysis Science & Technology* 2016, **6**, 4910.
31 R. Pellegrini, G. Leofanti, G. Agostini, E. Groppo, M. Rivallan and C. Lamberti, *Langmuir* 2009, **25**, 6476.
32 G. Panaccione, I. Vobornik, J. Fujii, D. Krizmancic, E. Annese, L. Giovanelli, F. Maccherozzi, F. Salvador, A. De Luisa, D. Benedetti, A. Gruden, P. Bertoch, F. Polack, D. Cocco, G. Sostero, B. Diviacco, M. Hochstrasser, U. Maier, D. Pescia, C. H. Back, T. Greber, J. Osterwalder, M. Galaktionov, M. Sancrotti and G. Rossi, *Review of Scientific Instruments* 2009, **80**, 043105.
33 M. Smith, L. Scudiero, J. Espinal, J.-S. McEwen and M. Garcia-Perez, *Carbon* 2016, **110**, 155.
34 D. Colognesi, M. Celli, F. Cilloco, R. J. Newport, S. F. Parker, V. Rossi-Albertini, F. Sacchetti, J. Tomkinson and M. Zoppi, *Applied Physics a-Materials Science & Processing* 2002, **74**, S64.
35 O. Arnold, J. C. Bilheux, J. M. Borreguero, A. Buts, S. I. Campbell, L. Chapon, M. Doucet, N. Draper, R. Ferraz Leal, M. A. Gigg, V. E. Lynch, A. Markvardsen, D. J. Mikkelson, R. L. Mikkelson, R. Miller, K. Palmen, P. Parker, G. Passos, T. G. Perring, P. F. Peterson, S. Ren, M. A. Reuter, A. T. Savici, J. W. Taylor, R. J. Taylor, R. Tolchenov, W. Zhou and J. Zikovsky, *Nuclear Instruments and Methods in Physics Research Section A: Accelerators, Spectrometers, Detectors and Associated Equipment* 2014, **764**, 156.
36 http://www.chimet.com/en/catalyst
37 G. Agostini, E. Groppo, A. Piovano, R. Pellegrini, G. Leofanti and C. Lamberti, *Langmuir* 2010, **26**, 11204.
38 J. R. Anderson and K. C. Pratt, *Introduction to Characterization and Testing of Catalysts*; Academic Press: Sydney, Australia, **1986**.
39 G. Agostini, R. Pellegrini, G. Leofanti, L. Bertinetti, S. Bertarione, E. Groppo, A. Zecchina and C. Lamberti, *The Journal of Physical Chemistry C* 2009, **113**, 10485.
40 G. Prelazzi, M. Cerboni and G. Leofanti, *Journal of Catalysis* 1999, **181**, 73.
41 E. Groppo, G. Agostini, A. Piovano, N. B. Muddada, G. Leofanti, R. Pellegrini, G. Portale, A. Longo and C. Lamberti, *Journal of Catalysis* 2012, **287**, 44.
42 G. Agostini, C. Lamberti, R. Pellegrini, G. Leofanti, F. Giannici, A. Longo and E. Groppo, *ACS Catalysis* 2014, **4**, 187.
43 J. S. Noh and J. A. Schwarz, *Carbon* 1990, **28**, 675.
44 S. Biniak, G. Szymański, J. Siedlewski and A. Świtkowski, *Carbon* 1997, **35**, 1799.
45 T. T. P. Cheung, *Journal of Applied Physics* 1984, **55**, 1388.
46 J. Diaz, G. Paolicelli, S. Ferrer and F. Comin, *Physical Review B* 1996, **54**, 8064.
47 H. Estrade-Szwarckopf, *Carbon* 2004, **42**, 1713.
48 S. L. Feng, Y. G. Yang, L. Li, D. S. Zhang, X. M. Yang, S. Bai, H. H. Xia, L. Yan, P. Huai and X. T. Zhou, *Journal of Applied Physics* 2015, **117**.
49 S. Lizzit, L. Petaccia, A. Goldoni, R. Larciprete, P. Hofmann and G. Zampieri, *Physical Review B* 2007, **76**.
50 D. Pantea, H. Darmstadt, S. Kaliaguine and C. Roy, *Applied Surface Science* 2003, **217**, 181.
51 D. Q. Yang and E. Sacher, *Langmuir* 2006, **22**, 860.
52 R. Blume, D. Rosenthal, J.-P. Tessonnier, H. Li, A. Knop-Gericke and R. Schlögl, *ChemCatChem* 2015, **7**, 2871.
53 A. C. Ferrari, S. E. Rodil and J. Robertson, *Physical Review B* 2003, **67**, 155306.
54 A. Centrone, L. Brambilla, T. Renouard, L. Gherghel, C. Mathis, K. Müllen and G. Zerbi, *Carbon* 2005, **43**, 1593.
55 D. R. Dreyer, S. Park, C. W. Bielawski and R. S. Ruoff, *Chem. Soc. Rev.* 2010, **39**, 228.
56 B. Konkena and S. Vasudevan, *J. Phys. Chem. Lett.* 2012, **3**, 867.
57 A. A. Ibrahim, A. Lin, F. Zhang, K. M. AbouZeid and M. S. El-Shall, *ChemCatChem* 2017, **9**, 469.
58 It is worth noticing that absorption bands in similar position could be compatible also with nitro groups, that have been claimed to form via nitration of the aromatic rings. However, in our case we exclude the presence of nitro groups because we did not detect nitrogen by means of any technique, and in particular by elementary analysis, EDX and XPS. .
59 P. W. Albers, J. Pietsch, J. Krauter and S. F. Parker, *Physical Chemistry Chemical Physics* 2003, **5**, 1941.
60 A. Piovano, A. Lazzarini, R. Pellegrini, G. Leofanti, G. Agostini, S. Rudic, A. L. Bugaev, C. Lamberti and E. Groppo, *Advances in Condensed Matter Physics* 2015, **2015**, 803267.
61 Note that some changes are observed in the very low frequency region, where the riding vibrations (i.e. C–C torsion modes of the carbon atoms at the edge of the sp^2 fragment, which indirectly cause a substantial movement of the hydrogen atoms) contribute to the spectrum, as well as COOH functional groups. Apparently, the treatment in HNO_3 causes the disappearance of part of the bands observed in the spectrum of **1a**. However, a deeper analysis of this spectral region would require the collection of less noisy spectra.
62 T.-Y. Chung, C.-S. Tsao, H.-P. Tseng, C.-H. Chen and M.-S. Yu, *Journal of Colloid and Interface Science* 2015, **441**, 98.
63

Graphical Abstract